Talanta 115 (2013) 394–400

Contents lists available at SciVerse ScienceDirect

Talanta

journal homepage: www.elsevier.com/locate/talanta

Resolving antibody–peptide complexes with different ligand stoichiometries reveals a marked affinity enhancement through multivalency

Jianhao Wang [a,b,1], Pengju Jiang [a,1], Lin Qiu [a], Cheli Wang [a], Jiang Xia [b,*]

[a] School of Pharmaceutical Engineering and Life Science, Changzhou University, Changzhou 213164, Jiangsu, China
[b] Department of Chemistry, The Chinese University of Hong Kong, Shatin, Hong Kong, China

ARTICLE INFO

Article history:
Received 28 March 2013
Received in revised form
25 May 2013
Accepted 30 May 2013
Available online 5 June 2013

Keywords:
Antibody–peptide interaction
Ligand stoichiometry
Capillary electrophoresis
Multivalency
Anti-FLAG antibody

ABSTRACT

Natural antibodies adopt multivalent constructs to effect superior binding affinities with their antigens. Notwithstanding that the structure of antibodies have been well understood, how antibodies harness multivalency effect to achieve superior binding affinity toward the antigens still remains unclear. Such investigation is often hampered by the difficulty in resolving receptor-ligand complexes with different stoichiometries in the binding solution, especially when the ligand is a small molecule or a short peptide. Here we employed a unique anti-FLAG™ mAb M2 and FLAG™ peptides system, together with fluorescence detection coupled capillary electrophoresis (CE-FL) to reveal how M2 achieves exceptional high affinity with FLAG peptides through multivalency. Complexation of fluorescently labeled FLAG™ peptides with M2 leads to a pronounced mobility shift of the fluorescent peak in CE. Remarkably, CE-FL rendered a base-line separation of 1:1 and 1:2 M2–FLAG™ complexes, allowing the quantification of different M2–FLAG™ species. The quantitative analysis leads to a detailed dissection of the first (functional affinity) and second binding affinities (intrinsic affinity) between M2 and $FLAG_1$ peptide. The marked difference (10^3–10^4 fold) between these two affinities indicated that multivalency effect plays a key role for M2 to achieve highly efficient binding to FLAG™ peptides.

1. Introduction

Multivalent binding interactions, i.e. binding interactions with stoichiometries other than 1, play a pivotal role in bio-recognitions both in solution and at interfaces [1–3]. For example, an IgG antibody (Immunoglobulin *G*) harboring two antigen-binding sites can bind to two antigens (or more specifically, epitope peptides) independently, representing a bivalent binding interaction [4]. How antibodies adopt such multivalent constructs to achieve superior binding affinity toward their specific antigens still remains unsolved. The difficulty lies, at least partially, in chromatographic resolution of antibody–peptide complexes with different ligand stoichiometries in solution, because the differences in molecular weights, surface shape, and hydrophobicity between the two are very subtle. Considering that an IgG antibody weighs around 150 K Da, for epitope peptides of molecular weights around 2 K Da (~15 residues), the 1:2 IgG–peptide complex differs from the 1:1 complex by less than 1% in molecular weight and surface area. Such a minute difference poses a significant challenge in the separation of these two based on their sizes, charges, or hydrophobicity, and inevitably calls for methods with outstanding separation capability. Most analytical and physiochemical methods that are widely applied to antibody–antigen interaction studies do not meet this challenge, such as surface plasmon resonance (SPR) [5–7], enzyme-linked immunosorbent assay (ELISA) [8], FRET-based homogeneous immunoassay [9], isothermal calorimetry (ITC) [10], and high perfomance size exclusion chromatography (HPSEC) [10–14] and others [15–17]. SPR and ELISA require the immobilization of one of the binding partners, often the antibodies. The lack of precise control of the density and orientation of immobilized antibodies on the surface might result in heterogeneity in the binding interaction and cause considerable deviation from the binding interaction in solution. Nonetheless, determination of antibody–antigen binding stoichiometry was achieved through theoretical simulation of the resonance signals in SPR [5,6]. ITC measures the overall thermal effect upon binding, providing little information on the details of complex formation. HPSEC represents a solution-based method that can chromatographically separate free protein, free peptide and protein–peptide complexes, but it fails to provide finer resolution. Mass spectrometry effectively separates different species by m/z ratio with the finest resolution, thus applicable to antibody–antigen

* Corresponding author. Tel.: +852 39436165; fax: +852 26035057.
E-mail address: jiangxia@cuhk.edu.hk (J. Xia).
[1] These authors contributed equally to this work.

0039-9140/$ - see front matter © 2013 Elsevier B.V. All rights reserved.
http://dx.doi.org/10.1016/j.talanta.2013.05.070

binding studies. Robinson and others used a combination of nanoflow-electrospray ionization and time-of-flight mass spectrometry to analyze antibody–antigen interactions and successfully resolved complexes of different stoichiometies [18]. Its success notwithstanding, sophisticated instruments and special techniques are required, thus not generally applicable to average labs. Recently, affinity capillary electrophoresis (ACE), a.k.a. immunoaffinity capillary electrophoresis, has found great success in determining binding constants and stoichiometry for antibody–antigen interactions [19]. Binding constants corresponding to the formation of multivalent antibody–antigen complexes with different stoichiometries were calculated based on the change in electrophoretic mobility [19–23]. Fluorescence detection coupled capillary electrophoresis coupled with (CE-FL) features a facile setup, highly sensitive fluorescence detection, fast analysis, micro litter-volume sample consumption and high resolution, and thus has been widely used in the separation of biomolecules [24–26] and bioanalysis [27–29]. Recently, we utilized a home-built CE-FL instrument to resolve HLA-DQ2 proteins complexed with different peptides, highlighting the superior separation capacity of CE-FL on subtly different protein–peptide complexes [30]. This success inspired us to seek a chromatographic separation of 1:1 and 1:2 IgG–peptide complexes by CE-FL. We envision that the chromatographic resolution of antibody–peptide complexes of different ligand stoichiometries will shed light on the role of antibody's multivalent construction in bio-recognition.

Here, we chose FLAG™ peptides (FLAGs) and anti-FLAG™ M2 monoclonal antibody (M2) as a model system to probe their interaction by CE-FL. FLAG™ tags are designed peptide tags for detection, identification, capturing, and purification of recombinant proteins [31,32]. The small size of FLAG™ peptides ensures a minimal steric hindrance to facilitate the formation of 1:2 M2–FLAG complex. More importantly, the peptide sequence is highly negatively charged, rendering them the optimal candidate for capillary electrophoretic studies, analogous to 2,4-dinitrophenyl ligands [20]. M2 is an IgG_1 monoclonal antibody isolated from a murine cell culture that tightly binds to FLAG™ fusion proteins, which has found wide application in immunoaffinity chromatography [31–35]. SPR analyses revealed that M2 binds to a surface-immobilized FLAG peptide SGDYKDDDDK with a very low K_d of 6.5 nM [36]. Considering that M2 bound with FLAG tagged proteins on cell surface with 1:1 stoichiometry [37], this remarkable K_d value indicates an exceptionally high apparent affinity between M2 and FLAG peptides. On the other hand, based on the crystal structure of monovalent M2 Fab, the antigen-binding site of M2 only accommodates a tetrapeptide DYKD [38]. This rather small contact between protein and peptide cannot unriddle the mechanism of its high binding affinity. Then a possible explanation is multivalency-assisted affinity enhancement, i.e. notwithstanding a single fork of M2 binds FLAG with moderate affinity, the divalent structure of IgG results in significant enhancement of the apparent affinity. In this report, we present a resolution of the first and second peptide binding steps by CE-FL and evidence that multivalency does play a key role in such a protein–peptide interaction.

2. Experimental

2.1. Materials and methods

Anti-FLAG™ M2 monoclonal antibody was purchased from Sigma-Aldrich. Rink Amide-ChemMatrix® resin was from Matrix Innovation (Montreal, Canada). HPLC-grade acetonitrile, diethyl ether, dichloromethane (DCM) and N,N-dimethylformamide (DMF) were from Labscan (Thailand). N,N-diisopropylethylamine (DIPEA), and trifluoroacetic acid (TFA) were from Meryer Technologies Co., Ltd. (Shenzhen, China). 2-(1H-benzotriazol-1-yl)-1,1,3,3-tetramethyluronium hexafluorophosphate (HBTU) were from Chem-Impex International Inc. (USA). Fmoc-protected amino acids, N-hydroxybenzotriazole (HOBt) and 1-Ethyl-3-[3–dimethylaminopropyl]carbodiimide hydrochloride (EDC) were obtained from GL Biochem Ltd. (Shanghai, China). 5(6)-carboxyfluorescein (fl) was purchased from Invitrogen. Cy5 free acid was a gift from Prof. Chaitan Khosla at Stanford University.

2.2. Solid phase peptide synthesis

All the peptides were synthesized by solid phase peptide synthesis technique based on the 9-fluorenylmethoxycarbonyl (Fmoc) chemistry using Rink Amide-ChemMatrix® resin, and a 5-fold excess of amino acid activated by one equivalent of 1:1 HBTU/HOBt in DMF. Each coupling step lasted for 30 min. The Fmoc group was deprotected by piperidine/DMF (20% v/v) for 30 min. Peptides were labeled at their N-termini while still attached to the resin with either fl or Cy5 free acid (3 fold molar excess) in the presence of equal molar EDC and DIPEA in DMF over night. Peptides were cleaved from the resin by a cleavage cocktail of trifluoroacetic acid (TFA), ethanedithiol, water, and triisopropylsilane (94:2.5:2.5:1, v/v) for 2 h at room temperature. The peptides were then precipitated in ice-cold diethyl ether, pelleted by centrifugation, dissolved in water, purified by semi-preparative reserve-phase HPLC, and lyophilized. The molecular weights of the peptides were confirmed by MALDI-TOF mass spectrometry (Fig. S1 in Supporting information).

Analytical reversed-phase HPLC was performed on a Vydac (218TP54) RP-HPLC column (C18, 5 μm, 4.6 mm ID × 250 mm, Alltech Associates, Inc., USA) on a LC-2010A HPLC system (Shimadzu, Kyoto, Japan). Solvent A was 0.1% (v/v) TFA in water, and solvent B was 0.1% (v/v) TFA in acetonitrile. A linear gradient of increasing percentage of solvent B was set. Flow rate was set at 1 mL/min. Preparative HPLC was performed on a Vydac (218TP510) RP-HPLC column (C18, 5 μm, 10 mm ID × 250 mm, Alltech Associates, Inc., USA) with a flow rate of 3 mL/min. Cy5-labeled peptides and fl-labeled peptides were purified and the concentration was quantified using UV–vis absorption (ε_{650}=250,000 M^{-1} cm^{-1} for Cy5, ε_{492}=74,600 M^{-1} cm^{-1} for fl).

2.3. CE-FL analyses

CE-FL analyses were carried out on a home-built system, consisting of a high voltage supply (0–30 kV) (Shanghai Nuclear Research Institute, China), a fused silica capillary with an inner diameter (ID) of 75 μm (Yongnian Optical Fiber Factory, Hebei, China) and an inverted fluorescence microscope (IX71, Olympus, Japan) equipped with a 100 W mercury lamp (OSRAM HBO 103w/2 Mercury Arc Lamp), an excitation filter (BP 420 ± 20 nm), a dichromatic mirror (DM 455) and a fiber optic spectrometer (QE65000, Ocean Optics, USA) attached to the side port (Fig. S2). Briefly, a short length of the coating around a capillary was removed to expose a transparent region for fluorescence detection. The capillary was then positioned on the sample stage the microscope, allowing the adjustment of the objective lens to focus on the transparent region. The fluorescent signal emitted through the transparent region within the area of detection window will be transmitted to a fiber optic spectrometer that is connected to the U-CMAD3 adapter on the side of the microscope, allowing the recording of the emission spectra. The effective length (length from injection to the detection window) was set to be 35 cm. Capillaries were primed by rinsing with 0.1 M HCl, pure water, 0.1 M NaOH, pure water and electrophoretic buffer sequentially for 20 min prior to use. Samples were hydrodynamically injected into capillary at 10 cm height for 10 s. The capillary was washed with running buffer for 10–15 min before each run to ensure the reproducibility. All electropherograms were acquired at room temperature.

2.4. M2–peptide binding experiments

M2 antibody was first diluted to 2.7 μM with 10 mM borate buffer (pH 7.4). 5 μL $FLAG_1$-Cy5, $FLAG_1$-fl or $FLAG_2$-Cy5 peptides of various concentrations and 5 μL M2 were mixed with the final concentration of M2 being 1.35 μM, and incubated at room temperature for 30 min. The resulting mixtures were injected into a capillary, and the eluates were monitored at appropriate excitation and emission wavelengths.

Peak areas corresponding to the M2–$FLAG_1$ complexes M2–$(FLAG_1\text{-}Cy5)_1$, M2–$(FLAG_1\text{-}Cy5)_2$ and free peptides were integrated using Origin 7.5. The fractions of each species among the overall amount of input fluorescent peptide were calculated as the ratio of peak area over the sum of all the fluorescent species M2–$(FLAG_1\text{-}Cy5)_1$, M2–$(FLAG_1\text{-}Cy5)_2$ and free $FLAG_1$-Cy5 peptide. The area fractions were then converted to concentrations based on the assumption that the integrated areas of fluorescent peaks represent the concentrations of respective fluorescent species in the binding mixture. Dissociation constants K_{D1} and K_{D2} were then calculated based on the concentrations. Fig. S3 shows one example of the calculation process.

2.5. Peptide competition assay

M2 were first mix with $FLAG_1$-Cy5 at 1:1 ratio (1.35 μM) to form a pre-bound state of M2–$(FLAG_1\text{-}Cy5)_1$. Then 40 fold excess of $FLAG_3$ (54 μM) was mix with M2–$(FLAG_1\text{-}Cy5)_1$ complex. The dissociation of the M2–$(FLAG_1\text{-}Cy5)_1$ complex was then monitored by CE-FL.

3. Results and discussion

3.1. CE analysis of fluorescently labeled FLAG™ peptides

The fluorescence detection coupled capillary electrophoresis system (CE-FL) was set up by assembling a fluorescent microscope, a capillary electrophoresis setup, and an optic spectrometer as previously described (See details in Section 2.1 and Fig. S2) [30,39]. This facile setup features the high resolution separation by the capillary electrophoresis, multi-channel excitation of the microscope, and the full-spectrum detection of the spectrometer to allow the simultaneous recording of the fluorescence spectrum of each peak from capillary electrophoresis [30,39]. Importantly, in contract to mass spectrometers and commercial CEs, this is a relatively budget-efficient solution of setting up a CE in labs already equipped with a fluorescent microscope.

We first synthesized different variants of FLAG™ peptides through Fmoc solid phase peptide synthesis and examined their capillary electropherograms. We chose FLAG™ variants DYKDDDDA, DYKADDDK and DYKDADDK (termed $FLAG_1$, $FLAG_2$ and $FLAG_3$ respectively) which have different binding properties with M2 [32]. K8A variant $FLAG_1$ DYKDDDDA and D5A variant $FLAG_3$ DYKDADDK had similar binding affinities as the parental peptide DYKDDDDK, whereas the D4A modification in $FLAG_2$ DYKADDDK totally abolished its binding with M2, indicated by ELISA analysis [32]. FLAG™ variants labeled with racemic green fluorescent dye 5-(and -6)-carboxyfluorescein (fl) and a blue Cyanine dye Cy5 migrated as symmetric peaks with narrow peak widths in CE-FL (Fig. 1 and Table 1). Despite the same amino acid sequence and similar overall molecular weights, $FLAG_1$-fl migrated more slowly than $FLAG_1$-Cy5 (942 s) and showed split peaks at 1025 s and 1069 s. Peak splitting can be ascribed to the 5- and 6- isomers of fl label on $FLAG_1$-fl (on the contrary, Cy5 is a single compound, Fig. 1). The base-line resolution of subtly different 5-fl and 6-fl labeled $FLAG_1$-fl hinted at the superior separation capability of our CE-FL setup, in which peptides having the same sequence with only very small differences in chemical structure or surface shape could be separated in CE. Therefore, subtle difference in stereochemistry of the fluorophore can be reflected in the electrophoretic migration of labeled peptides. Evidently, Cy5-labeled peptides showed very narrow peak widths, in contrast to fl labeled $FLAG_1$.

3.2. CE-FL analysis of M2–FLAG1-FL binding interaction

The interaction between epitope peptide $FLAG_1$-fl and M2 antibody was then attempted utilizing our CE setup. Incubation of $FLAG_1$-fl with M2 at 2:1 ratio resulted in a significant change in the elctropherogram (Fig. 2). Two new peaks at t_m of 506 s (P3) and 910 s (780–920 s, P4) emerged. P3, with the lowest mobility, corresponds to the 1:1 complex M2–$(FLAG_1\text{-}fl)_1$, and P4 corresponds to M2–$(FLAG_1\text{-}fl)_2$. Integration of the peaks estimated that 9.4% of the total peptide input are in free unbound form, with the majority 81.3% forming M2–$(FLAG_1\text{-}fl)_2$ complex and the remaining 9.3% as 1:1 complex. This first binding experiment showed that $FLAG_1$ efficiently binds to the first antigen-binding site of M2, while the occupation of the second antigen-binding site is cumbersome, suggesting that M2 binds with $FLAG_1$ with high *functional affinity* but with relatively low *intrinsic affinity* at the single binding site (the detailed quantification is shown below).

3.3. Confirming the epitope binding specificity

Having demonstrated that $FLAG_1$-fl binds to M2 by CE-FL, we then examined the binding specificity of the synthetic FLAG™

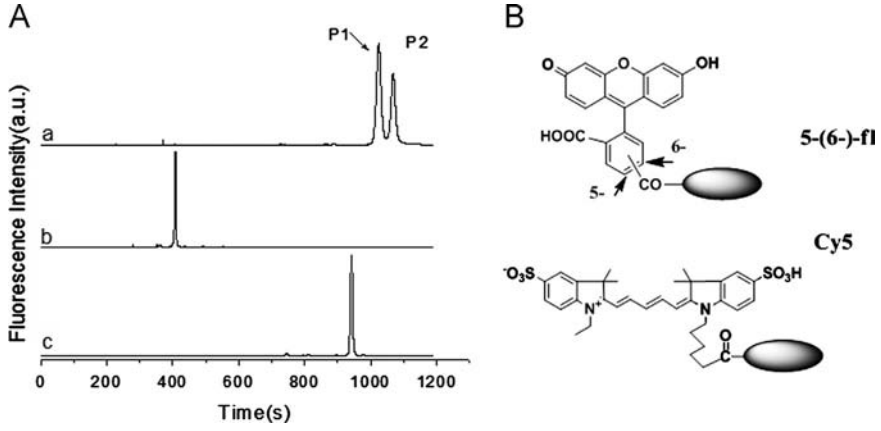

Fig. 1. Electropherograms of fluorescent FLAG™ variants. (A) a, $FLAG_1$-fl; b, $FLAG_2$-Cy5; c, $FLAG_1$-Cy5. CE condition: sodium phosphate buffer (pH 7.17, 47 mM Na_2HPO_4, 20 mM KH_2PO_4) at 10 kV. (a, λ_{ex}=480 nm; b, c, λ_{ex}=530 nm). (B) Structures of the fluorescent dyes used.

Table 1
CE parameters of FLAG™ variants and M2–FLAG complexes.

Entries	Sequence	t_m (s)	μ_{ep} (10^{-4} cm^2/V s)[a]
$FLAG_1$-fl	fl-DYKDDDDA	1025	−3.34
		1069	−3.43
$FLAG_1$-Cy5	Cy5-DYKDDDDA	942	−3.16
$FLAG_2$-Cy5	Cy5-DYKADDDK	410	−0.27
$FLAG_3$	DYKDADDK		
M2–$(FLAG_1$-fl$)_1$		506	−1.24
M2–$(FLAG_1$-fl$)_2$		780–920	−3.08
M2–$(FLAG_1$-Cy5$)_1$		500	−1.19
M2–$(FLAG_1$-Cy5$)_2$		810	−3.092
		912	

[a] μ_{ep}, effective electrophoretic mobility. Electroosmotic flow was measured using rhodamine B as the neutral marker. Electroosmotic mobility = 5.39×10^{-4} cm^2/V s.

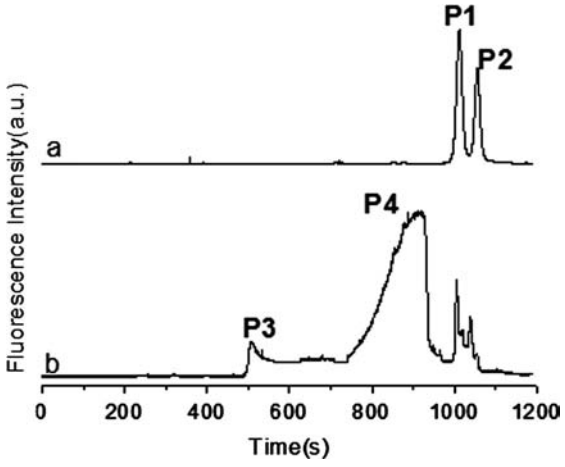

Fig. 2. Electropherograms of M2 and $FLAG_1$-fl peptide binding (a, $FLAG_1$-fl; b, M2 +$FLAG_1$-fl, M2: $FLAG_1$-fl = 1:2). CE condition: Sodium phosphate buffer (pH 7.17, 47 mM Na_2HPO_4, 20 mM KH_2PO_4) at 10 kV (λ_{ex} = 480 nm).

peptides. As revealed in previous characterization of M2–FLAG binding by ELISA, the displacement of the first D in $FLAG_1$ diminished its binding to M2 antibody [32]. The same result was seen here, as mixing M2 with $FLAG_2$-Cy5 at 1:2 ratio caused little change in the electropherogram (Fig. 3A). This indicates that the binding between $FLAG_1$-fl and M2 we observed in CE-FL is sequence dependent, ruling out non-specific adhesion between the two. To further confirm that $FLAG_1$ binds to the antigen-binding sites of M2 antibody, we performed a competition study using a non-fluorescent D5A variant $FLAG_3$ (DYKDADDK), which has different peptide sequence as $FLAG_1$ but similar binding affinity to M2. An M2–$(FLAG_1$-Cy5$)_1$ 1:1 complex were first allowed to form by mixing equimolar $FLAG_1$-Cy5 with M2. The M2–$(FLAG_1$-Cy5$)_1$ complex at t_m 500 s, was clearly resolvable from the free $FLAG_1$-Cy5 peptide at t_m 942 s (Fig. 3B, Table 1). Non-fluorescent $FLAG_3$ in excess effectively competed $FLAG_1$-Cy5 off from the antigen-binding sites of M2 and reverted the M2–$(FLAG_1$-Cy5$)_1$ complex to free $FLAG_1$-Cy5 (Fig. 3B). The competition experiment between different epitopes confirms that variants of FLAG™ peptide of similar affinity bind competitively to M2 at the antigen-binding sites, therefore the binding is specific.

3.4. Examining the details of M2–FLAG1-Cy5 binding interaction

The above explorations set the stage for stepwise examination of the binding interaction between $FLAG_1$-Cy5 and M2. First, the marked difference in electrophoretic properties of $FLAG_1$-fl and $FLAG_1$-Cy5 was revealed, leading to the choice of $FLAG_1$-Cy5 for the further characterization. Second, the M2–FLAG binding interaction is sequence-specific and competitive to different FLAG™ peptides. Thirdly and the most importantly, the M2–FLAG complexes with 1:1 and 1:2 stoichiometries are well separable from free peptide in CE-FL.

We first set the boundary conditions. $FLAG_1$-Cy5 exhibited a peak at 942 s, which defines the boundary at the highest mobility because binding to M2 reduces its mobility (Table 1). As shown above, 1:1 M2:$FLAG_1$-Cy5 ratio results in almost stoichiometrical formation of M2–$(FLAG_1$-Cy5$)_1$ species. Therefore, M2–$(FLAG_1$-Cy5$)_1$ complex formed at 1:1 M2:$FLAG_1$-Cy5 ratio represents the other boundary with the lowest mobility, with t_m of 506 s. As an IgG molecule binds to at most two $FLAG_1$ epitope peptides, these two boundaries bracket M2−$(FLAG_1$-Cy5$)_n$ complex species with stoichiometry ratio n between 1 and 2.

We then dissected the divalent M2–$FLAG_1$ binding interaction into two steps (Scheme 1). The first step is the binding of the first antigen to M2 in a stoichiometric manner, with the corresponding dissociation constant defined as K_{D1}. At 1:1 M2:$FLAG_1$-Cy5 ratio, integration of the peak areas indicates that the free $FLAG_1$-Cy5 peak represents about 0.7% of the total fluorescent signals, or 0.01 μM in solution (total peptide input is 1.35 μM) (Fig. 4, trace a), therefore K_{D1} can be calculated to be about 10^{-10} M (0.1 nM) based on Equation 1 in Scheme 1. As the 1:1 complex M2–$(FLAG_1$-Cy5$)_1$ is still receptive to FLAG™ peptides at the other antigen-binding site in M2, adding one more equivalent of $FLAG_1$-Cy5 peptide to the 1:1 solution allows for the second antigen-binding step (Scheme 1). K_{D2} was defined as the dissociation constant of $FLAG_1$ binding to the second antigen-binding site on M2 after the first antigen-binding site being occupied (Equation 2 in Scheme 1). Therefore, the first and second binding affinities K_{D1} and K_{D2} represent the *functional affinity* (also referred as *avidity*) [40] of M2–$FLAG_1$ binding interaction, and the *intrinsic affinity* (or *affinity* for comparison with avidity) of $FLAG_1$ binding to individual antigen-binding site on M2, respectively.

At 1:2 M2:$FLAG_1$-Cy5 ratio, between the two boundaries of free peptide and 1:1 M2–FLAG complex, two peaks emerge, with t_m at 810 and 912 s respectively. Consistent with the capillary electrophoretic studies of M2–$FLAG_1$-fl binding at 1:2 ratio (Fig. 2), both peaks P2 and P2′ can be ascribed as M2–c$FLAG_1$-Cy5$)_2$ complexes with alternative structures. At saturating concentrations of $FLAG_1$-Cy5 (FLAG:M2 = 8:1, trace d in Fig. 4), the M2–$FLAG_1$-Cy5$)_1$ peak disappeared while the ratio of the heights of the 810 and 912 s peaks remains the same as the cases in FLAG:M2 of 2:1 and 4:1 (traces b and c in Fig. 4). Therefore, the two peaks represent M2–h$FLAG_1$-Cy5$)_2$ complex with different structures, so the peak areas are combined. Based on the peak integration as shown in Fig. S3 in supporting information as well as calculation according to Equation 2 in Scheme 1, K_{D2} was calculated to be 0.35 μM in M2:$FLAG_1$-Cy5 ratio of 1:2 (trace b in Fig. 4), and 2.76 μM in M2:$FLAG_1$-Cy5 ratio of 1:4 (trace c in Fig. 4). Despite the discrepancy in exact number due to the overlap between M2–$FLAG_1$-Cy5$)_2$ complex peak and free peptide peak, K_{D2} can be safely estimated to be in the order of 10^{-6} M. The assignment of P2′ as an M2–a$FLAG_1$-Cy5$)_2$ complex with alternative structure is arguable. Nevertheless, taking P2′ out from the calculation does not qualitatively change the conclusion. Integrating the peak areas from 820–932 s yields a K_{D2} of 0.28 μM in M2:$FLAG_1$-Cy5 ratio of 1:2, and 2.17 μM in M2:$FLAG_1$-Cy5 ratio of 1:4 (Fig. S4 in supporting information). Qualitatively, at 1:2 ratio with $FLAG_1$ peptide of 2.7 μM and M2 of 1.35 μM, a significant amount of free $FLAG_1$ peptide remains, also indicating the second binding step has an intrinsic affinity in 10^{-6} M(μM) range. Therefore, in contrast to K_{D1} at 10^{-10} M, K_{D2} is about 10^3–10^4 fold higher. The marked difference between K_{D1} and K_{D2} indicates that the binding of the first $FLAG_1$ peptide to M2 is very efficient, while the binding of the second $FLAG_1$ peptide to M2 is cumbersome, in the case that the concentrations of antibody and its antigen are in μM range. As the two identical antigen-

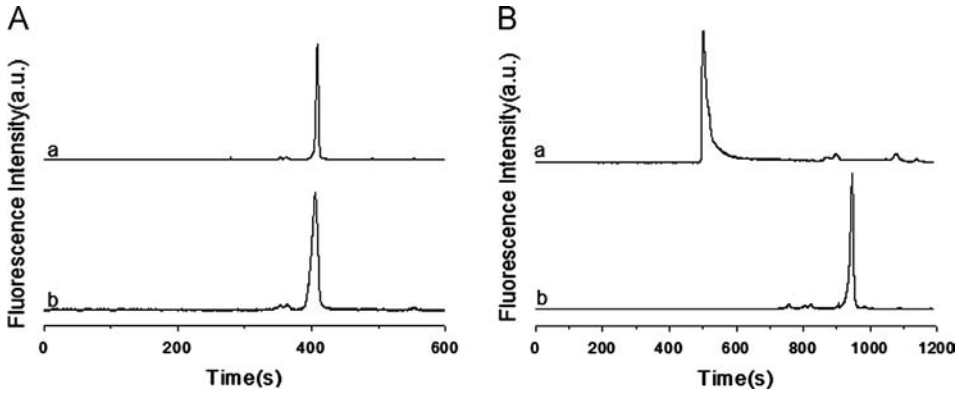

Fig. 3. M2–$FLAG_1$-Cy5 displaced by $FLAG_3$. (A) Electropherograms of M2 and $FLAG_2$-Cy5 peptide binding (a, $FLAG_2$-Cy5 only; b, M2+$FLAG_2$-Cy5, M2:$FLAG_2$-Cy5=1:2). (B) Electropherograms of M2–$(FLAG_1\text{-Cy5})_1$ complex (a) and the complex after $FLAG_3$ displacement (b). CE condition: Sodium phosphate buffer (pH 7.17, 47 mM Na_2HPO_4, 20 mM KH_2PO_4) at 10 kV (λ_{ex}=530 nm).

$$K_{D.1} = \frac{[FLAG_1\text{-Cy5})]_{free} \bullet [M2]_{free}}{[M2-(FLAG_1\text{-Cy5})_1]} \quad (1)$$

$$K_{D.2} = \frac{[M2-(FLAG_1\text{-Cy5})_1] \bullet [FLAG_1\text{-Cy5}]_{free}}{[M2-(FLAG_1\text{-Cy5})_2]} \quad (2)$$

Scheme 1. Definition of the equilibrium constants.

binding sites of the Fab fractions of intact IgG are far apart by ~150 Å based on the crystal structure [41], and the FLAG™ peptide is very small (8 residues, < 30 Å), steric hindrance is negligible in the second binding step, i.e. the binding of the second epitope peptide to the empty antigen-binding site of the M2–$(FLAG_1\text{-Cy5})_1$ complex is not hindered by the first epitope peptide. Excluding steric effect, the 10^3–10^4 fold difference between K_{D1} and K_{D2} can only be attributed to multivalency effect of divalent antibody. From the association aspect of view, although each single antigen-binding site of M2 has moderate intrinsic affinity to $FLAG_1$ peptide, two antigen-binding sites in close proximity greatly increases the "local concentration" of the binding sites thus greatly enhanced the change for a peptide to bind to one of the binding sites. From the dissociation aspect of view, the dissociated $FLAG_1$ peptide is still in the proximity of two antigen-binding sites instead of one site, which greatly increases its chance to re-bind to M2 before diffusing away. Such a gain of overall binding efficacy by a factor of 10^3–10^7 reflects an important mechanism for an antibody to acquire superior binding affinity through multivalency effect [4]. The high functional affinity achieved through bivalent binding of two sites with moderate intrinsic affinity also significantly contributes to the potency of antibodies as therapeutic agents [42].

3.5. Discussion

Therefore in sharp contrast to the previously reported IgG: small molecule interaction (K_2/K_1~4, none cooperative binding) based on ACE [20], our work demonstrated that there exists a marked multivalency in the M2–FLAG™ binding interaction. Multivalency-assisted affinity enhancement has also been observed in other binding pairs [43–47]. For example, anti-polysaccharide IgG antibodies bound to the ligand 10^2–10^3 times tighter than their monovalent counterparts, Fab fragment and single-chain variable fragments (scFvs) [43].

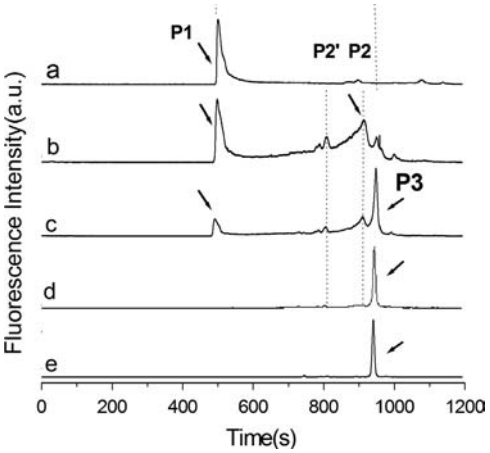

Fig. 4. Electropherograms of different ratios of $FLAG_1$-Cy5/M2 binding mixture: a, 1:1; b, 2:1; c, 4:1; d, 8:1; e, $FLAG_1$-Cy5 ([M2]=1.35 μM). CE condition: Sodium phosphate buffer (pH 7.17, 47 mM Na_2HPO_4, 20 mM KH_2PO_4) at 10 kV (λ_{ex}= 480 nm).

Several features distinguish our study from the previous studies of receptor–ligand interaction. Micromolar concentrations of M2 and FLAG peptide were mixed in the assay solutions. The high apparent binding affinity (K_{D1}~nM) leads to a nearly quantitative formation of M2–$(FLAG)_1$ complex. Such condition is different from those assayed by ACE, where normally interactions with μM K_D values were assayed at nM concentrations [19,20,48]. This difference leads to the observation of a discrete M2–$(FLAG)_1$ peak in our CE, unlike a mobility shift of receptor peak based on the concentration of the ligand in ACE. The formation of M2–$(FLAG)_2$ is much less efficient, corresponding to significant peak broadening. Thus, prudent selection of the experimental system and assay conditions gave us a unique chance to fully reveal the subtle details of this interaction.

Fast dissociation of antibody–antigen complexes with relatively low affinity during electrophoresis caused noticeable changes in their electropherograms in a pioneering work [49]. Correlation between electrophoretic migration and binding kinetics is also evident in our assay. It has been measured that the association rate of antibody–antigen interaction is in the range of 10^4 M^{-1} s^{-1} [50], so the dissociation rate of M2–$(FLAG_1\text{-Cy5})_1$ complex, k_{d1} is around 10^{-6} s^{-1}. As our assay requires a separation time of 10^2–10^3 s, dissociation of M2–$(FLAG_1\text{-Cy5})_1$ complex in capillary is negligible. On the contrary, since the second binding step (Step 2 in Scheme 1) is much weaker (K_{D2}~10^{-6} M), k_{d2} is around 10^{-2} s^{-1}. Dissociation of M2–$(FLAG_1\text{-Cy5})_2$ complex during electrophoresis is thus significant. This also explains while M2–$(FLAG_1\text{-Cy5})_1$

showed a discrete peak, M2–($FLAG_1$-Cy5)$_2$ species exhibited a rather broad peak on electropherograms.

This method is also generalizable to the study of other antibody–peptide interactions. Although a highly negatively charged ligand peptide, such as FLAG peptides is the prerequisite of successful separation, appending a Cy5-DDDD- sequence at terminus of the peptide outside the binding pocket meets the requirement without changing the binding properties [39]. Our work thus investigated antibody–peptide binding interaction from a unique angle, relying on the resolution of different antibody–peptide complexes to reveal a marked multivalency-assisted affinity enhancement.

The present study proves CE-FL to be a powerful method to resolve M2–FLAG™ complexes with different stoichiometries. At 1:1 ratio in μM range, more than 99% of $FLAG_1$-Cy5 bound to M2 to form M2–($FLAG_1$-Cy5)$_1$ complex, whilst the addition of the second equivalent of $FLAG_1$-Cy5 lead to only partial formation of M2–($FLAG_1$-Cy5)$_2$. This suggests that the second binding constant K_{D2} is about 10^3–10^4 fold higher than the first binding constant K_{D1}. Therefore the M2–FLAG™ binding interaction shows a marked multivalency effect, in sharp contrast to the previously reported IgG:small molecule interaction (K_2/K_1~4, none cooperative binding) based on ACE [20]. Multivalency-assisted affinity enhancement has also been observed in other binding pairs [43–47]. For example, anti-polysaccharide IgG antibodies bound to the ligand 10^2–10^3 times tighter than their monovalent counterparts, Fab fragment and single-chain variable fragments (scFvs) [43].

Several features distinguish our study from the previous studies of receptor–ligand interaction. Micromolar concentrations of M2 and FLAG peptide were mixed in the assay solutions. The high apparent binding affinity (K_{D1}~nM) leads to a nearly quantitative formation of M2–($FLAG$)$_1$ complex. Such condition is different from those assayed by ACE, where normally interactions with μM K_D values were assayed at nM concentrations [19,20,48]. This difference leads to the observation of a discrete M2–($FLAG$)$_1$ peak in our CE, unlike a mobility shift of receptor peak based on the concentration of the ligand in ACE. The formation of M2–($FLAG$)$_2$ is much less efficient, corresponding to significant peak broadening. Thus, prudent selection of the experimental system and assay conditions gave us a unique chance to fully reveal the subtle details of this interaction.

Fast dissociation of antibody–antigen complexes with relatively low affinity during electrophoresis caused noticeable changes in their electropherograms in a pioneering work [49]. Correlation between electrophoretic migration and binding kinetics is also evident in our assay. It has been measured that the association rate of antibody–antigen interaction is in the range of 10^4 M^{-1} s^{-1} [50], so the dissociation rate of M2–($FLAG_1$-Cy5)$_1$ complex, k_{d1} is around 10^{-6} s^{-1}. As our assay requires a separation time of 10^2–10^3 s, dissociation of M2–($FLAG_1$-Cy5)$_1$ complex in capillary is negligible. On the contrary, since the second binding step (Step 2 in Scheme 1) is much weaker (K_{D2}~10^{-6} M), k_{d2} is around 10^{-2} s^{-1}. Dissociation of M2–($FLAG_1$-Cy5)$_2$ complex during electrophoresis is thus significant. This also explains while M2–($FLAG_1$-Cy5)$_1$ showed a discrete peak, M2–($FLAG_1$-Cy5)$_2$ species exhibited a rather broad peak on electropherograms.

4. Conclusions

The present study proves CE-FL to be a powerful method to resolve M2–FLAG™ complexes with different stoichiometries. At 1:1 ratio in μM range, more than 99% of $FLAG_1$-Cy5 bound to M2 to form M2–($FLAG_1$-Cy5)$_1$ complex, whilst the addition of the second equivalent of $FLAG_1$-Cy5 lead to only partial formation of M2–($FLAG_1$-Cy5)$_2$. This suggests that the second binding constant K_{D2} is about 10^3–10^4 fold higher than the first binding constant K_{D1}. This method is also generalizable to the study of other antibody–peptide interactions. Although a highly negatively charged ligand peptide, such as FLAG peptides is the prerequisite of successful separation, appending a Cy5-DDDD- sequence at terminus of the peptide outside the binding pocket meets the requirement without changing the binding properties [39]. Our work thus investigated antibody–peptide binding interaction from a unique angle, relying on the resolution of different antibody–peptide complexes to reveal a marked multivalency-assisted affinity enhancement.

Acknowledgments

This work was supported by the Research Grants Council of Hong Kong (GRF grant CUHK 403711), the National Natural Science Foundation of China (Grant nos. 81201085, and 31100530) and the Science & Technology Support Program of Changzhou (Society Development) (No. CE20125052). This work was also supported by "A Project Funded by the Priority Academic Program Development of Jiangsu Higher Education Institutions".

Appendix A. Supplementary information

Supplementary data associated with this article can be found in the online version at http://dx.doi.org/10.1016/j.talanta.2013.05.070.

References

[1] L.L. Kiessling, J.E. Gestwicki, L.E. Strong, Angew. Chem. Int. Ed. 45 (2006) 2348–2368.
[2] W.B. Turnbull, Nat. Chem. 3 (2011) 267–268.
[3] J. Huskens, Curr. Opin. Chem. Biol. 10 (2006) 537–543.
[4] I. Kumagai, K Tsumoto, Antigen–antibody binding, Encyclopedia of Life Sciences, John Wiley & Sons, Ltd., Hoboken, NJ, USA, 2001.
[5] M. Oda, T. Azuma, Mol. Immunol. 37 (2000) 1111–1122.
[6] S. Lin, A.S. Lee, C.C. Lin, C.K. Lee, Curr. Proteomics 3 (2006) 271–282.
[7] M. Oda, N. Sato-Nakamura, T. Azuma, Anal. Biochem. 333 (2004) 365–371.
[8] F. Hardy, L. Djavadi-Ohaniance, M.E. Goldberg, J. Immunol. Methods 200 (1997) 155–159.
[9] T. Kreisig, R. Hoffmann, T. Zuchner, Anal. Chem. 83 (2011) 4281–4287.
[10] M.M. Pierce, C.S. Raman, B.T. Nall, Methods 19 (1999) 213–221.
[11] R.V. Joshi, J.A. Zarutskie, L.J. Stern, Biochemistry 39 (2000) 3751–3762.
[12] B.J. McFarland, J.F. Katz, A.J. Sant, C. Beeson, J. Mol. Biol. 350 (2005) 170–183.
[13] C.G. Sanny, J.A. Price, Anal. Biochem. 24 (1997) 7–14.
[14] D.J. Winzor, Anal. Biochem. 383 (2008) 1–17.
[15] A. Sadana, D. Sii, Biosens. Bioelectron. 7 (1992) 559–568.
[16] L. Tao, R.T. Kennedy, Electrophoresis 18 (1997) 112–117.
[17] T. Tu, M. Drăguşanu, B.A. Petre, D.L. Rempel, M. Przybylski, M.L. Gross, J. Am. Soc. Mass Spectrom. 21 (2010) 1660–1667.
[18] M.A. Tito, J. Miller, N. Walker, K.F. Griffin, E.D. Williamson, D. Despeyroux-Hill, R.W. Titball, C.V. Robinson, Biophys. J. 81 (2001) 3503–3509.
[19] W.L. Tseng, H.T. Chang, S.M. Hsu, R.J. Chen, S. Lin, Electrophoresis 23 (2002) 836–846.
[20] M. Mammen, F.A. Gomez, G.M. Whitesides, Anal. Chem. 67 (1995) 3526–3535.
[21] N.H. Heegaard, O.J. Bjerrum, Anal. Biochem. 195 (1991) 319–326.
[22] N.H. Heegaard, J. Chromatogr. A 680 (1994) 405–412.
[23] N.H. Heegaard, R.T. Kennedy, J. Chromatogr. B 768 (2002) 93–103.
[24] E.A.S. Doherty, R.J. Meagher, M.N. Albarghouthi, A.E. Barron, Electrophoresis 24 (2003) 34–54.
[25] M.F. Huang, Y.C. Kuo, C.C. Huang, H.T. Chang, Anal. Chem. 76 (2004) 192–196.
[26] J. Khandurina, N.A. Olson, A.A. Anderson, K.A. Gray, A. Guttman, Electrophoresis 25 (2004) 3117–3121.
[27] Y.Q. Li, J.H. Wang, H.L. Zhang, J. Yang, L.Y. Guan, H. Chen, Q.M. Luo, Y.D. Zhao, Biosens. Bioelectron. 25 (2010) 1283–1289.
[28] Y.Q. Li, L.Y. Guan, H.L. Zhang, J. Chen, S. Lin, Z.Y. Ma, Y.D. Zhao, Anal. Chem. 83 (2011) 4103–4109.
[29] X. Song, L. Li, H. Qian, N. Fang, J. Ren, Electrophoresis 27 (2006) 1341–1346.
[30] J. Wang, X. Jin, J. Liu, C. Khosla, J. Xia, Chem. Asian J. 7 (2012) 992–999.
[31] A. Einhauer, A. Jungbauer, J. Biochem. Biophys. Methods 49 (2001) 455–465.
[32] J.W. Slootstra, D. Kuperus, A. Plückthun, R.H. Meloen, Mol. Divers. 2 (1996) 156–164.
[33] A. Knappik, A. Plückthun, Biotechniques 17 (1994) 754–761.
[34] K.S. Prickett, D.C. Amberg, T.P. Hopp, Biotechniques 7 (1989) 580–589.
[35] L.S. Park, D. Friend, V. Price, D. Anderson, J. Singer, K.S. Prickett, D.L. Urdal, J. Biol. Chem. 264 (1989) 5420–5427.

[36] G.J. Wegner, H.J. Lee, R.M. Corn, Anal. Chem. 74 (2002) 5161–5168.
[37] D. Firsov, L. Schild, I Gautschi, A.M. Merillat, E. Schneeberger, B.C. Rossier, Proc. Natl. Acad. Sci. U.S.A 93 (1996) 15370–15375.
[38] T.P. Roosild, S. Castronovo, S. Choe, Acta Crystallogr. Sect. F Struct. Biol. Cryst. Commun. 62 (2006) 835–839.
[39] J. Wang, J. Xia, Anal. Chem. 83 (2011) 6323–6329.
[40] C.L. Hornick, F. Karush, Immunochemistry 9 (1972) 325–330.
[41] L.J. Harris, S.B. Larson, K.W. Hasel, A. McPherson, Biochemistry 36 (1997) 1581–1597.
[42] Y. Zhou, A.-L. Goenaga, B.D. Harms, H. Zou, J. Lou, F. Conrad, G.P. Adams, B. Schoeberl, U.B. Nielsen, J.D. Marks, Mol. Cancer Ther. 11 (2012) 1467–1476.
[43] S. Müller-Loennies, C.G. MacKenzie, S.I. Patenaude, S.V. Evans, P. Kosma, H. Brade, L. Brade, S. Narang, Glycobiology 10 (2000) 121–130.
[44] R. Zidovetzki, A. Licht, I. Pecht, Proc. Natl. Acad. Sci. USA 76 (1979) 5848–5852.
[45] R. Zidovetzki, A. Licht, I. Pecht, Mol. Immunol. 18 (1981) 491–497.
[46] S.J. Sucheck, A.L. Wong, K.M. Koeller, D.D. Boehr, K.-a. Draker, P. Sears, G.D. Wright, C.-H. Wong, J. Am. Chem. Soc. 122 (2000) 5230–5231.
[47] S.L. Mangold, M.J. Coninger, Org. Biomol. Chem. 4 (2006) 2458–2465.
[48] Y.-H. Chu, L.Z. Avila, J. Gao, G.M. Whitesides, Acc. Chem. Res. 28 (1995) 461–468.
[49] N.M. Schultz, R.T. Kennedy, Anal. Chem. 65 (1993) 3161–3165.
[50] G. Zhuang, Y. Katakura, T. Omasa, M. Kishimoto, K. Suga, J. Biosci. Bioeng. 92 (2001) 330–336.